Original Article
J. Korean Wood Sci. Technol. 2023, 51(5): 321-333
https://doi.org/10.5658/WOOD.2023.51.5.321

Journal of the Korean Wood Science and Technology
pISSN: 1017-0715 eISSN: 2233-7180
http://www.woodj.org

Cationized Lignin Loaded Alginate Beads for Efficient Cr(VI) Removal

Jungkyu KIM[1] · YunJin KIM[1] · Seungoh JUNG[1] · Heecheol YUN[1] · Hwanmyeong YEO[1,2] · In-Gyu CHOI[1,2] · Hyo Won KWAK[1,2,†]

ABSTRACT

In this study, lignin, a lignocellulosic biomass, was chemically modified to produce polyethyleneimine-grafted lignin (PKL) with maximum hexavalent chromium [Cr(VI)] adsorption capacity. Changes in the physicochemical properties due to the cationization of lignin were confirmed through elemental analysis, Fourier transform infrared spectroscopy, and moisture stability evaluation. Alginate (Alg) beads containing PKL (Alg/PKL) were prepared by incorporating cationic lignin into the Alg matrix to apply the prepared PKL in a batch-type water treatment process. The optimal Alg/lignin mixing ratio was selected to increase the Cr(VI) adsorption capacity and minimize lignin elution from the aqueous system. The selected Alg/PKL beads exhibited an excellent Cr(VI) removal capacity of 478.98 mg/g. Isothermal adsorption and thermodynamic analysis revealed that the Cr(VI) removal behavior of the Alg/PKL beads was similar to that of heterogeneous chemical adsorption. In addition, the bulk adsorbent material in the form of beads exhibited adsorption behavior in three stages: surface adsorption, diffusion, and equilibrium.

Keywords: lignin, cationization, Cr(VI), alginate, adsorbent

1. INTRODUCTION

Lignin is a major component of wood and is the second most abundant biomass source on Earth (Bang *et al*., 2022; Fatriasari *et al*., 2020; Iswanto *et al*., 2021; Lee *et al*., 2021; Watumlawar and Park, 2023). The lignin is mostly burned as an energy source in paper and pulping industries (Hwang *et al*., 2021). However, the unique aromatic structure of lignin and the existence of various functional groups, including hydroxyl groups, suggest the possibility of using lignin as a raw material for polymeric materials (Park *et al*., 2020). In addition, interest in the use of lignin in the field of organic materials is increasing, as the functional properties of lignin, such as antioxidant, antibacterial, and UV properties, have been discovered recently.

There are two strategies for utilizing lignin in the materials industry. First, lignin can be used as an additive by exploiting the functionality of raw lignin materials (Cahyani *et al*., 2023; Hwang and Oh, 2023; Min and

Date Received June 19, 2023, Date Revised July 12, 2023, Date Accepted July 25, 2023
[1] Department of Agriculture, Forestry and Bioresources, College of Agriculture & Life Sciences, Seoul National University, Seoul 08826, Korea
[2] Research Institute of Agriculture and Life Sciences, Seoul National University, Seoul 08826, Korea
[†] Corresponding author: Hyo Won KWAK (e-mail: bk0502@snu.ac.kr, https://orcid.org/0000-0003-1630-7210)

Um, 2017; Pawale *et al*., 2022). However, this method has the disadvantage that only a small amount of lignin can be used. Second, there is a method of utilizing a large amount of lignin by performing pretreatment and chemical modification to control its nonuniform physicochemical properties of lignin (Chen *et al*., 2021b; Sangian *et al*., 2018). In this regard, the value of lignin as a polymer material can be increased by implementing methods such as the organosolve process, controlling the molecular weight and functional groups of lignin through solvent fractionation, and imparting thermoplasticity through polymer grafting.

It has been known that lignin has excellent adsorption capacity for various harmful substances because it has an aromatic backbone capable of π–π bonding, aliphatic functional groups capable of hydrogen bonding, and oxygen-containing functional groups including phenolic hydroxyl groups (Ma *et al*., 2020). Kim *et al*. (2022) developed a lignin-based fibrous adsorbent for removing ionic dyes and confirmed that lignin exhibited excellent adsorption capacity for cationic dyes. However, because lignin mainly has anionic functional groups, such as carboxyl and hydroxyl groups, on its surface, it has a poor adsorption capacity for contaminants with negative charges, such as anionic dyes, chromium, and palladium compounds. In addition, most lignin-based adsorbents introduced thus far are composed of powdered lignin materials; therefore, it is difficult to apply them in batch or column processes for water treatment (Behboudi *et al*., 2021; Fu *et al*., 2019). In addition, because the use of adsorbents in the powder state requires an additional separation process for the adsorbents from contaminated water, conversion to bulky adsorbents, such as beads, fibers, and hydrogels, is essential.

In this study, the surface of lignin was chemically modified to maximize its adsorption capacity for anionic contaminants. Changes in the physicochemical properties of lignin due to cationization were confirmed through Fourier transform infrared spectroscopy (FTIR), elemental analysis, X-ray photoelectron spectroscopy (XPS) analysis, and lignin elution experiments in a water environment. In addition, a bead-type adsorbent with improved stability in a moist environment was prepared by incorporating cationized lignin into an alginate (Alg) matrix for utilization in a batch-type water treatment process and easy separation of the lignin-based adsorption material from contaminated water. Isothermal adsorption and adsorption kinetics analyses were performed to evaluate the hexavalent chromium [Cr(VI)] removal performance of cationized lignin-containing Alg beads and elucidate the Cr(VI) removal mechanism. Finally, the possibility of sustainable use of cationized lignin-containing Alg beads was evaluated through a reuse experiment.

2. MATERIALS and METHODS

2.1. Materials

Kraft lignin (KL) was kindly provided by Moorim P&P (Ulsan, Korea). Formaldehyde (37 wt%), polyethyleneimine (PEI, M_w ~800, branched), 1,5-diphenylcarbazide (≥ 98.0%), potassium dichromate (99.5%), sulfuric acid (95%–97%), calcium chloride (≥ 93.0%), and sodium Alg were purchased from Sigma-Aldrich (Yongin, Korea). Sodium hydroxide was purchased from Junsei Chemical (Tokyo, Japan).

2.2. Preparation of polyethyleneimine (PEI)-grafted lignin (PKL)

KL (5 g) and formaldehyde (1 g) were added to a 50 mL solution of 4 wt% PEI. The pH of the solution was adjusted to 10.0, and the mixture was reacted at 50℃ for 5 hours. After the reaction, the pH was lowered to 3.5 to precipitate the PKL. The obtained PKL was washed with distilled water (DW) until the washed water became neutral and then dried in an oven.

2.3. Characterization of polyethyleneimine (PEI)-grafted lignin (PKL)

The chemical structures of lignin before and after the introduction of PEI were compared using FTIR spectroscopy (Nicolet Summit FTIR Spectrometer, Thermo Fisher Scientific, Waltham, MA, USA) and XPS (Axis Supra, Kratos Analytical, Manchester, UK). FTIR spectra were recorded in the spectral range of 4,000−700 cm^{-1} with 64 scans and a scan resolution of 4 cm^{-1} in attenuated total reflectance mode. The atomic ratios of KL and PKL were assessed using an elemental analyzer (Flash EA 1112, Thermo Electron, Waltham, MA, USA). Lignin was mixed with 0.1 M HCl, NaOH, and DW and stirred at 150 rpm for 1 hour to evaluate the water stability of lignin according to pH. The dissolution of lignin in each solution was measured using a UV-vis spectrometer (OPTIZENTM POP, KLAB, Daejeon, Korea) at an absorbance of 280 nm wavelength (Singh *et al*., 2022), and calculated using Equation (1):

$$\text{Lignin dissolution } (\%) = \frac{A_a - A_t}{A_a} \times 100 \quad (1)$$

where A_a represents the absorbance of the solution when all the lignin has dissolved, and A_t is the absorbance of the solution after t min.

2.4. Preparation and characterization of alginate (Alg) beads containing polyethyleneimine (PEI)-grafted lignin (PKL)

Alg/PKL beads were prepared by the ionic gelation of Alg (Fig. 1). PKL was added to a 2 wt% sodium Alg solution to prepare various ratios (1:0, 1:0.5, 1:1.0, 1:1.5, and 1:2.0) of the Alg/PKL solutions. The resulting Alg/PKL solution was added dropwise to a 2 wt% CaCl2 solution using a syringe pump (KDS 100 Legacy, KD Scientific, Holliston, MA, USA). The distance between the surface of the CaCl2 solution and the needle tip was fixed at 5 cm. The sodium ions surrounding the Alg were replaced with calcium ions through a double replacement reaction, and the Alg solidified into beads. The cross-linked Alg/PKL beads were washed twice with DW. The morphological properties of Alg/PKL beads was analyzed using digital camera (Galaxy S10e, Samsung, Suwon, Korea) and field emission scanning electron microscopy (FE-SEM, SUPRA 55VP, Carl Zeiss, Baden-Württemberg, Germany).

2.5. Cr(VI) adsorption study of alginate (Alg)/polyethyleneimine (PEI)-grafted lignin (PKL) beads

A 1,000 mg/L Cr(VI) solution was prepared using $Cr_2K_2O_7$ and diluted to concentrations ranging from 10 to 550 mg/L. Alg/PKL beads (50 mg) were added to 50 mL of a Cr(VI) aqueous solution at various concentrations and stirred at 4 g during the adsorption experiment. After adsorption, the concentration of Cr(VI) remaining in the solution was evaluated using a colorimetric method using 1,5-diphenylcarbazide (Lace *et al*., 2019). For this evaluation, 45 mL of DW, 100 μL of Cr(VI) aqueous solution, 10% (v/v) sulfuric acid, and 1% (w/v) 1,5-diphenylcarbazide solution were mixed for 30 s. The absorbance of the mixed solution was measured using UV-vis spectrophotometry at a wavelength of 540 nm (Hasija *et al*., 2021). The Cr(VI)-adsorption capacity of the Alg/PKL beads was calculated using Equation (2):

$$q_e = \frac{(C_0 - C_e) \times V}{M} \quad (2)$$

where C_0 and C_e are the initial and equilibrium concentrations of aqueous Cr(VI) solution (mg/L), respectively, V denotes the volume (L) of the Cr(VI) aqueous

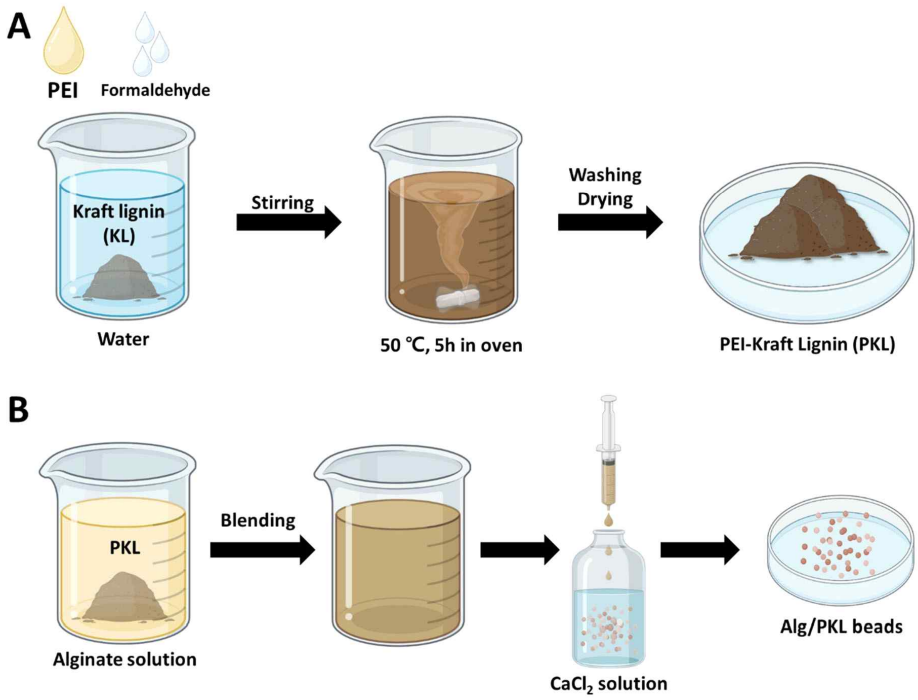

Fig. 1. Scheme of (A) PKL and (B) Alg/PKL bead preparation. PEI: polyethyleneimine, Alg: alginate.

solution, and M is the mass (g) of the adsorbent.

The Cr(VI) adsorption performance of the Alg/PKL beads was evaluated under various adsorption parameters, including different concentrations and time conditions. The adsorption isotherms and kinetic analyses were conducted for each condition. For the adsorption isotherm analysis, the equilibrium concentrations of Cr(VI) in the solution at different initial concentrations were determined, and the data were fitted to various isotherm models, such as Langmuir or Freundlich, to understand the adsorption behavior and determine the maximum adsorption capacity. For the adsorption kinetics analysis, the change in Cr(VI) concentration over time was measured, and kinetic models, such as Pseudo-first-order or Pseudo-second-order kinetics, were applied to determine the rate of adsorption and the mechanisms involved.

The reusability of the Alg/PKL beads was assessed using a 100 mg/L Cr(VI) solution. The Alg/PKL beads, which had adsorbed Cr(VI), were desorbed using a 0.1 M NaOH solution to remove Cr(VI), and then they were added back into a fresh 100 mg/L Cr(VI) solution. The adsorption–desorption cycle was repeated five times to evaluate the reusability of the Alg/PKL beads.

3. RESULTS and DISCUSSION

3.1. Preparation and characterization of polyethyleneimine (PEI)-grafted lignin (PKL)

PEI was introduced to impart a cationic functional group to the lignin surface, and phenol-formaldehyde was used as a crosslinking agent. FTIR analysis was performed to observe the changes in the chemical pro-

perties of lignin after cationization. As shown in Fig. 2(A), in the case of PKL, amide bonds at 1,650 cm^{-1} and C-N bonds at 1,125 cm^{-1} were newly created, through which PEI was covalently introduced into the lignin surface and contained a large number of amine groups (Wei *et al*., 2021). Cationization by the introduction of

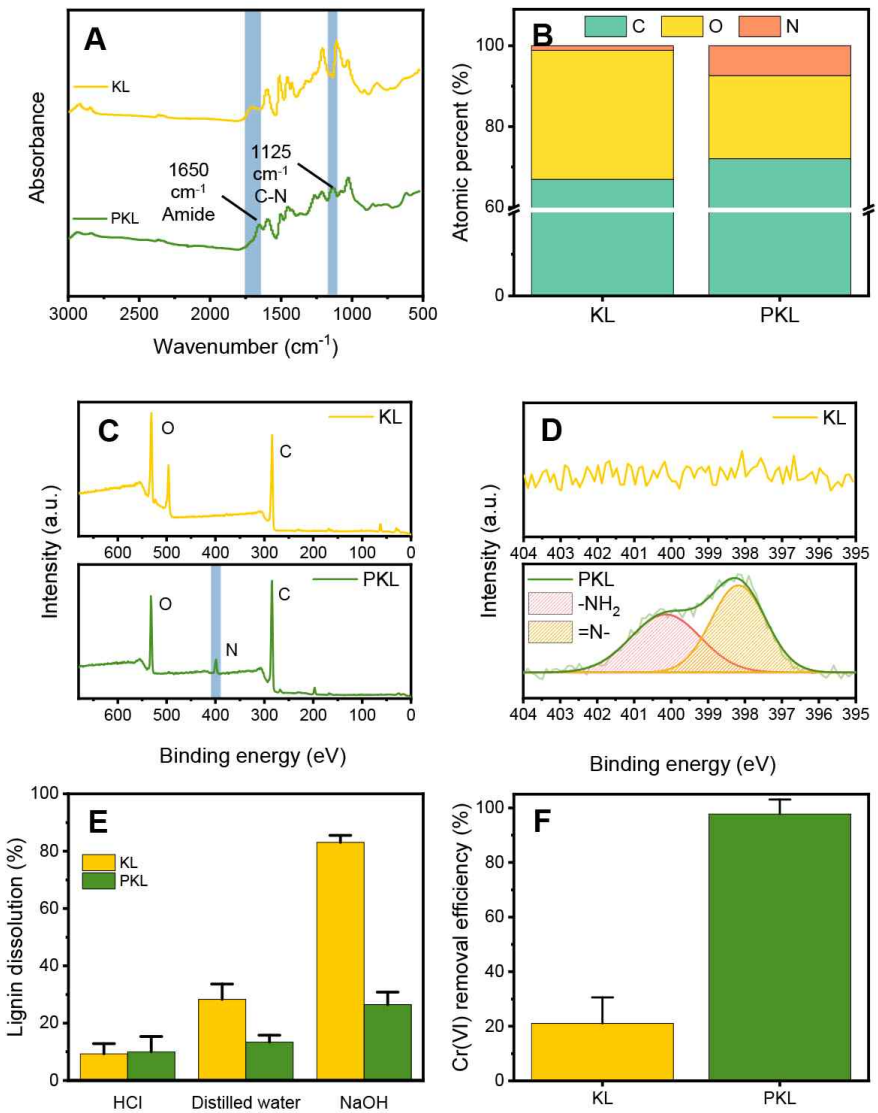

Fig. 2. Characterization of KL and PKL. (A) FTIR spectra, (B) atomic ratio, (C, D) XPS spectra, (E) lignin dissolution in aqueous condition, and (F) Cr(VI) removal efficiency of KL and PKL. KL: kraft lignin, PKL: polyethyleneimine-grafted lignin, FTIR: Fourier transform infrared spectroscopy, XPS: X-ray photoelectron spectroscopy.

PEI was easily confirmed by a change in composition [Fig. 2(B)]. KL was composed of 67% carbon, 31.9% oxygen, and 1.1% trace nitrogen. In contrast, the nitrogen content increased to 7.4% for cationized lignin, which was attributed to the presence of PEI on the surface. This increase in nitrogen content was also observed in the XPS spectrum, and the introduced amine functional group was confirmed through the high-resolution N 1s spectrum [Fig. 2(C) and (D)]. Nitrogen peaks were not observed in KL, while N- at 398.2 eV and $-NH_2$ functional group peaks at 401.2 eV were observed for cationized lignin (Zhu *et al*., 2014). Stability in various pH environments is essential in water treatment adsorbents for sustainable utilization through excellent removal efficiency and repeated reuse. In the case of KL, chemical and physical crosslinking processes are required because lignin elution occurs easily via dissolution in an alkaline environment. Elution experiments were conducted under acidic, DW, and basic conditions to examine the effects of the introduction of PEI and the crosslinking process using phenol-formaldehyde on the water stability of PKL [Fig. 2(E)]. In the case of KL, the dissolution rate was less than 30% under acidic and DW conditions, but showed a high dissolution rate of 83% under basic conditions owing to the solubility of KL. However, in the case of PKL, a crosslinking process involving covalent bonding with phenol-formaldehyde was performed, and the elution rate in the base decreased to 26.5%. In addition, the dissolution characteristics of lignin could be effectively controlled by incorporating an additional Alg matrix into the prepared PKL. An adsorption experiment in a 100 mg/L Cr(VI) solution was conducted to examine the effect of cationization on the Cr(VI) removal characteristics of lignin [Fig. 2(F)]. KL showed a Cr(VI) removal efficiency close to 20%, while PKL showed a Cr(VI) removal efficiency close to 100%. This is because the lignin surface exhibits cationization properties through the introduction of a large number of amine groups, thereby maximizing the electrostatic attraction with the chromate anion (Li *et al*., 2018).

3.2. Preparation of cationized lignin containing alginate (Alg) beads

Generally, Alg gelation by adding polyvalent ions, including divalent ions, is a simple process. Calcium-induced gelation is the most popular gelation method for Alg, and it has been shown that an “egg box” structure appears due to a specific and strong interaction between the G block (α-L-guluronic acid) of Alg and Ca^{2+} (Alnaief *et al*., 2011). Beads of various Alg/PKL ratios were prepared to select the Alg/PKL ratio capable of maximizing the adsorption capacity of PKL via cationization and minimizing the elution of lignin. In the Fig. 3(A), it was found that Alg/lignin beads were formed up to a 1:2.0 (Alg:lignin) ratio, even with the addition of PKL, indicating that PKL was well incorporated into the Alg three-dimensional matrix. The presence or absence of lignin elution was examined under batch-type adsorption conditions according to the amount of lignin added, and the results are shown in Fig. 3(B). Even when 150% lignin was added compared to Alg, no lignin elution was observed; however, when 200% lignin was added, destruction of beads and elution of lignin were observed in a physically stirred environment. The Cr(VI) removal capacity of the adsorption material was evaluated based on the amount of PKL added. As shown in Fig. 3(C), the Cr(VI) removal capacity increased as the addition amount of PKL increased, and in the case of Alg/PKL beads with 150% addition, an excellent Cr(VI) removal capacity of 537.6 mg/g was observed. However, when 200% lignin was added, no noticeable increase in adsorption capacity was observed, which is thought to be the result of bead disintegration and lignin elution. To confirm the morphology of the Alg/lignin beads with cationized lignin, FE-SEM images of the beads lyophilized using liquid nitrogen were obtained, and the results

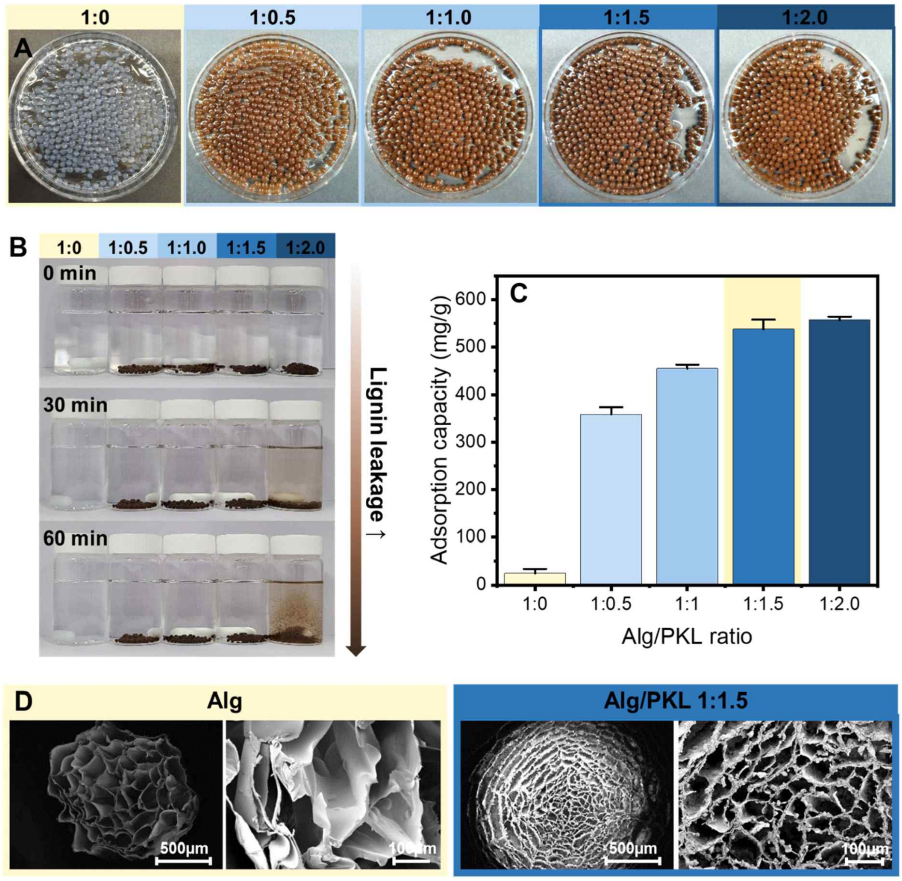

Fig. 3. Characterization of Alg and Alg/PKL beads. (A) Optical images of Alg beads with various PKL concentrations, (B) lignin leakages of Alg/PKL beads, (C) Cr(VI) removal efficiency of Alg/PKL beads prepared according to the ratio of Alg and PKL. (D) FE-SEM images of Alg and Alg/PKL beads selected as the optimal ratio. Alg: alginate, PKL: polyethyleneimine-grafted lignin, FE-SEM: field emission scanning electron microscopy.

are shown in Fig. 3(D). It showed the pure Alg beads having a diameter of 800 μm and a pore structure of 100−200 μm. In the case of Alg/lignin beads with 150% added, the size increased to an average diameter of 1,100 μm, which is due to the increase in viscosity according to the addition of lignin. Meanwhile, the pore size was also converted to a dense pore structure with a size of 50−100 μm, and PKL formed microparticles surrounding the Alg network structure. Overall, the amount of added lignin that could minimize lignin loss while maximizing the cationized lignin adsorption capacity was 150%. Therefore, an Alg/lignin ratio of 1:1.5 was selected as the optimal mixing condition and used for additional adsorption experiments.

3.3. Cr(VI) removal characteristics of polyethyleneimine (PEI)-grafted lignin (PKL) containing alginate (Alg) beads

The change in adsorption capacity according to the

initial Cr(VI) concentration was evaluated to determine the Cr(VI) removal performance of the prepared cationized lignin-containing Alg beads. As shown in the adsorption isotherms, the adsorption capacity of the lignin-containing Alg beads increased as the initial Cr(VI) concentration increased. This is because the interaction between the surface of the adsorbent and the adsorbate becomes more active as the adsorbate concentration in the limited contaminated water increases. The obtained results were fitted by applying the Langmuir and Freundlich models (Duman *et al*., 2020; Kwak *et al*., 2015), which are representative isothermal adsorption models commonly used to describe the interactions between adsorbents and adsorbates. The adsorption isotherm data were fitted using the Langmuir and Freundlich linear models by applying the following Equations (3) and (4):

$$\frac{1}{q_e}=\frac{1}{K_L q_{\max}}\times\frac{1}{C_e}+\frac{1}{q_{\max}} \tag{3}$$

$$\log(q_e)=\log(K_f)+\frac{1}{n}\log(C_e) \tag{4}$$

Equation (3) represents the linear equation for the Langmuir adsorption isotherm, and Equation (4) represents the linear equation for the Freundlich adsorption isotherm. In the equations, q_e represents the adsorption capacity at equilibrium, K_L is the Langmuir constant, q_{max} is the maximum adsorption capacity, K_f is the Freundlich constant, and 1/n is the Freundlich exponent of nonlinearity. The adsorption constants obtained from the Langmuir and Freundlich adsorption isotherm equations are presented in Table 1. As shown in Fig. 4(A) and (B), the Freundlich model showed better agreement than the Langmuir model, indicating that the removal behavior of Cr(VI) was heterogeneous. The maximum adsorption capacity of the Langmuir monolayer, obtained by applying the Langmuir model, is a representative performance comparison index for adsorbents. The q_{max} value of the Alg beads containing cationized lignin was 478.98 mg/g, which was the result of synergistic effects due to the cationic modification of lignin and its incorporation into the three-dimensional Alg network structure.

Table 1. Adsorption isotherm parameters of Cr(VI) on Alg/PKL beads

Parameter	Value	R^2
Langmuir isotherm		
q_{max} (mg/g)	478.98	0.924
K_L (L/mg)	0.03348	
Freundlich isotherm		
K_f	34.75	0.993
1/n	0.398	

Alg: alginate, PKL: polyethyleneimine-grafted lignin.

Representative kinetic models, pseudo-first and pseudo-second models, were applied to the results obtained to investigate the adsorption mechanism in more detail. The linear Equations (5) and (6) for the pseudo-first- and pseudo-second-order kinetics models are as follows:

$$\log(q_e-q_t)=\log(q_e)-\frac{k_1}{2.303}\times t \tag{5}$$

$$\frac{t}{q_t}=\frac{1}{k_2 q_e^2}+\frac{1}{q_e}\times t \tag{6}$$

where t is the adsorption time, k_1 is the rate constant of the pseudo-first-order kinetics, and k_2 is the rate constant of the pseudo-second-order kinetics. The adsorption kinetic constants obtained by fitting are listed in Table 2. As shown in Fig. 4(C) and (D) and Table 2, both the pseudo-first and pseudo-second models showed high agreement, indicating that both physical and chemical adsorption were involved in the removal

Table 2. Cr(VI) adsorption kinetic parameters of Alg/PKL beads

C_0 (mg/L)	Pseudo-first order			Pseudo-second order		
	k_1 (h^{-1})	q_e (mg/g)	R^2	k_2 (g/mg/h)	q_e (mg/g)	R^2
1,000	1.66	228.54	0.957	2.29×10^{-3}	436.68	0.998

Alg: alginate, PKL: polyethyleneimine-grafted lignin.

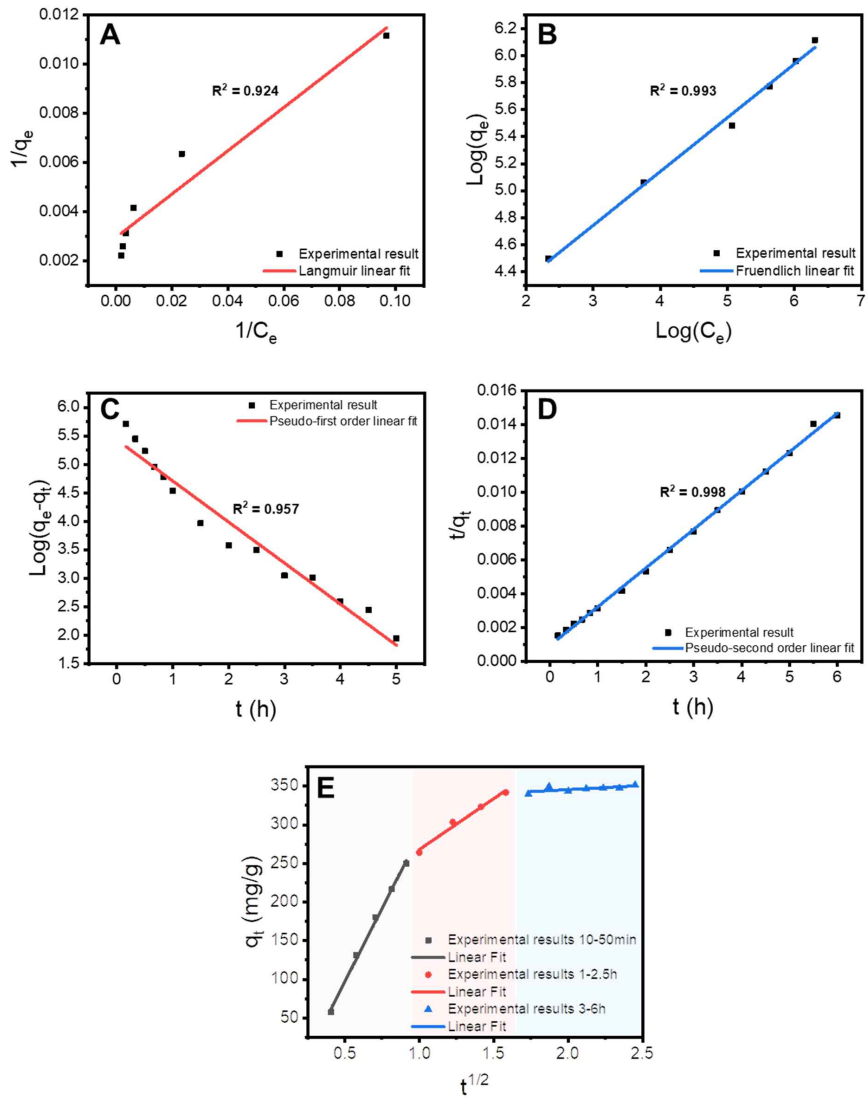

Fig. 4. Cr(VI) adsorption analysis results of Alg/PKL beads fitted with (A, B) adsorption isotherm, (C, D) adsorption kinetics, and (E) intra-particle diffusion model. Alg: alginate, PKL: polyethyleneimine-grafted lignin.

process of Cr(VI). The R^2 value for the pseudo-second-order model was 0.998, indicating an exceptionally good fit. Most cationically modified biomass-based adsorption materials are more suitable for the pseudo-second-order model (Kwak *et al*., 2020), indicating that the chemical-adsorption-based Cr(VI) removal mechanism is more strongly expressed. The adsorption kinetics results confirmed that a chemical bond was formed between the surface of the Alg beads containing cationized lignin and Cr(VI) contaminants (Chen *et al*., 2021a).

An adsorption experiment was conducted in a 1,000 mg/L Cr(VI) solution, and the change in adsorption capacity over time was measured to understand the principle of Cr(VI) removal behavior of the prepared lignin-based adsorbent. As shown in Fig. 4(E), the Cr(VI) adsorption behavior of Alg/PKL beads can be divided into three stages. In the first stage, the Cr(VI) ions diffuse from the bulk solution to the external surface of the adsorbent. Subsequently, the Cr(VI) ions that reached the external surface of the adsorbent underwent intraparticle diffusion and penetrated the interior of the particle. Finally, they reach the internal active sites of the adsorbent. The adsorption behavior of the Alg/PKL beads demonstrated the typical adsorption process of porous adsorbents. This observation was consistent with the FE-SEM image in Fig. 3(D).

3.4. Regeneration efficiency

Designing an optimal desorption process during adsorption to ensure continuous reusability is essential. The PKL-containing Alg beads adsorbed with Cr(VI) were immersed in 0.1 M NaOH to perform a desorption process, and repeated adsorption and desorption experiments were conducted to evaluate the reuse efficiency. In the initial one-time reuse environment, the reuse efficiency was close to 90%, as shown in Fig. 5. However, as the adsorption number increased, the continuous Cr(VI) adsorption efficiency decreased. After five reuse cycles, a low reuse efficiency of 46.6% was observed. This is because an alkaline environment, which is a desorption environment, can induce swelling of the Alg beads, and additional dissolution of Alg can also occur (Zhuang *et al*., 2016). For this reason, the desorption of Cr(VI) adsorbed in the basic environment and the elution of lignin occurs, and the adsorption efficiency decreases according to the number of reuses. Therefore, when an additional crosslinking process capable of minimizing the loss of Alg in a basic environment is proposed, it is believed that the reuse efficiency can also be improved.

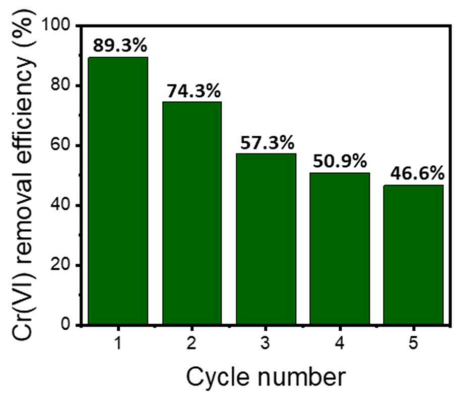

Fig. 5. Regeneration efficiency of Alg/PKL beads as Cr(VI) adsorbents. Alg: alginate, PKL: polyethyleneimine-grafted lignin.

4. CONCLUSIONS

In this study, lignin, a component of lignocellulosic biomass, was cationically modified and processed into beads, which strengthened its interaction with anionic chromate ions, to develop an adsorption material to remove Cr(VI). Using cationic PEI as a functional material and phenol-formaldehyde as a crosslinking agent, a large number of amine groups could be introduced to the surface of lignin, and the water stability was also increased due to crosslinking. However, when lignin was

incorporated into the Alg matrix, the amount of lignin required to maximize Cr(VI) removal while minimizing the loss of lignin was found to be 150% of the weight of Alg. The Alg beads containing the addition of cationized lignin showed an excellent Cr(VI) maximum removal capacity of 478.98 mg/g, owing to the cationic modification of lignin and its successful incorporation into the Alg network and pore structure. However, the efficiency decreased rapidly as the number of reuses increased in the reuse experiment, which was due to the structural instability of Alg under basic conditions, that is, the desorption environment of Cr(VI). Therefore, the potential use of lignin in the water treatment field will expand if a lignin incorporation technology with improved structural stability that guarantees stability under acid/base conditions, which is the adsorption/desorption condition of Cr(VI), is developed in the future.

CONFLICT of INTEREST

No potential conflict of interest relevant to this article was reported.

ACKNOWLEDGMENT

This study was conducted with the support of the 'R&D Program for Forest Science Technology (2020215 B10-2222-AC01)' and 'R&D Program for Forest Science Technology (2020224D10-2222-AC02)' provided by the Korea Forest Service (Korea Forestry Promotion Institute).

REFERENCES

Alnaief, M., Alzaitoun, M.A., García-González, C.A., Smirnova, I. 2011. Preparation of biodegradable nanoporous microspherical aerogel based on alginate. Carbohydrate Polymers 84(3): 1011-1018.

Bang, J., Kim, J., Kim, Y., Oh, J.K., Yeo, H., Kwak, H.W. 2022. Preparation and characterization of hydrophobic coatings from carnauba wax/lignin blends. Journal of the Korean Wood Science and Technology 50(3): 149-158.

Behboudi, G., Shayesteh, K., Tavakkoli Yaraki, M., Ebrahimi, H.A., Moradi, S. 2021. Optimized synthesis of lignin sulfonate nanoparticles by solvent shifting method and their application for adsorptive removal of dye pollutant. Chemosphere 285: 131576.

Cahyani, N., Yunianti, A.D., Suhasman, Pangestu, K.T.P., Pari, G. 2023. Characteristics of bio pellets from spent coffee grounds and pinewood charcoal based on composition and grinding method. Journal of the Korean Wood Science and Technology 51(1): 23-37.

Chen, N., Cao, S., Zhang, L., Peng, X., Wang, X., Ai, Z., Zhang, L. 2021a. Structural dependent Cr(VI) adsorption and reduction of biochar: Hydrochar versus pyrochar. Science of the Total Environment 783: 147084.

Chen, X., Pizzi, A., Zhang, B., Zhou, X., Fredon, E., Gerardin, C., Du, G. 2021b. Particleboard bio-adhesive by glyoxalated lignin and oxidized dialdehyde starch crosslinked by urea. Wood Science and Technology 56: 63-85.

Duman, O., Polat, T.G., Diker, C.Ö., Tunç, S. 2020. Agar/κ-carrageenan composite hydrogel adsorbent for the removal of methylene blue from water. International Journal of Biological Macromolecules 160: 823-835.

Fatriasari, W., Nurhamzah, F., Raniya, R., Laksana, R.P.B., Anita, S.H., Iswanto, A.H., Hermiati, E. 2020. Enzymatic hydrolysis performance of biomass by the addition of a lignin based biosurfactant. Journal of the Korean Wood Science and Technology 48(5): 651-665.

Fu, Y., Liu, X., Chen, G. 2019. Adsorption of heavy metal sewage on nano-materials such as titanate/TiO_2 added lignin. Results in Physics 12: 405-411.

Hasija, V., Raizada, P., Singh, P., Verma, N., Khan,

A.A.P., Singh, A., Selvasembian, R., Kim, S.Y., Hussain, C.M., Nguyen, V.H., Le, Q.V. 2021. Progress on the photocatalytic reduction of hexavalent Cr (VI) using engineered graphitic carbon nitride. Process Safety and Environmental Protection 152: 663-678.

Hwang, J.W., Oh, S.W. 2023. Mechanical properties and density profile of ceramics manufactured from a board mixed with sawdust and mandarin peels. Journal of the Korean Wood Science and Technology 51(2): 98-108.

Hwang, U.T., Bae, J., Lee, T., Hwang, S.Y., Kim, J.C., Park, J., Choi, I.G., Kwak, H.W., Hwang, S.W., Yeo, H. 2021. Analysis of carbonization behavior of hydrochar produced by hydrothermal carbonization of lignin and development of a prediction model for carbonization degree using near-infrared spectroscopy. Journal of the Korean Wood Science and Technology 49(3): 213-225.

Iswanto, A.H., Tarigan, F.O., Susilowati, A., Darwis, A., Fatriasari, W. 2021. Wood chemical compositions of raru species originating from Central Tapanuli, North Sumatra, Indonesia: Effect of differences in wood species and log positions. Journal of the Korean Wood Science and Technology 49(5): 416-429.

Kim, Y., Park, J., Bang, J., Kim, J., Kim, J.H., Hwang, S.W., Yeo, H., Choi, I.G., Kwak, H.W. 2022. Highly persistent lignocellulosic fibers for effective cationic dye pollutant removal. ACS Applied Polymer Materials 4(8): 6006-6020.

Kwak, H.W., Kim, M.K., Lee, J.Y., Yun, H., Kim, M.H., Park, Y.H., Lee, K.H. 2015. Preparation of bead-type biosorbent from water-soluble *Spirulina platensis* extracts for chromium (VI) removal. Algal Research 7: 92-99.

Kwak, H.W., Lee, H., Lee, K.H. 2020. Surface-modified spherical lignin particles with superior Cr(VI) removal efficiency. Chemosphere 239: 124733.

Lace, A., Ryan, D., Bowkett, M., Cleary, J. 2019. Chromium monitoring in water by colorimetry using optimised 1,5-diphenylcarbazide method. International Journal of Environmental Research and Public Health 16(10): 1803.

Lee, H., Kim, S., Park, M.J. 2021. Specific surface area characteristic analysis of porous carbon prepared from lignin-polyacrylonitrile copolymer by activation conditions. Journal of the Korean Wood Science and Technology 49(4): 299-314.

Li, Y., Zhu, H., Zhang, C., Cheng, M., He, H. 2018. PEI-grafted magnetic cellulose for Cr(VI) removal from aqueous solution. Cellulose 25: 4757-4769.

Ma, H., Li, T., Wu, S., Zhang, X. 2020. Effect of the interaction of phenolic hydroxyl with the benzene rings on lignin pyrolysis. Bioresource Technology 309: 123351.

Min, C.H., Um, B.H. 2017. Effect of process parameters and kraft lignin additive on the mechanical properties of miscanthus pellets. Journal of the Korean Wood Science and Technology 45(6): 703-719.

Park, S.Y., Choi, J.H., Cho, S.M., Choi, J.W., Choi, I.G. 2020. Structural analysis of open-column fractionation of peracetic acid-treated kraft lignin. Journal of the Korean Wood Science and Technology 48(6): 769-779.

Pawale, S., Kalia, K., Alshammari, S., Cronin, D., Zhang, X., Ameli, A. 2022. Deep eutectic solvent-extracted lignin as an efficient additive for entirely biobased polylactic acid composites. ACS Applied Polymer Materials 4(8): 5861-5871.

Sangian, H.F., Sehe, M.R., Tamuntuan, G.H., Zulnazri, Z. 2018. Utilization of saline solutions in the modification of lignocellulose from Champaca wood. Journal of the Korean Wood Science and Technology 46(4): 368-379.

Singh, A., Kumar, R., Maurya, A., Chowdhary, P., Raj, A. 2022. Isolation of functional ligninolytic *Bacillus aryabhattai* from paper mill sludge and its lignin degradation potential. Biotechnology Reports 35:

e00755.

Watumlawar, E.C., Park, B.D. 2023. Effects of precipitation pH of black liquor on characteristics of precipitated and acetone-fractionated kraft lignin. Journal of the Korean Wood Science and Technology 51(1): 38-48.

Wei, Y., Salih, K.A.M., Hamza, M.F., Fujita, T., Rodríguez-Castellón, E., Guibal, E. 2021. Synthesis of a new phosphonate-based sorbent and characterization of its interactions with lanthanum (III) and terbium (III). Polymers 13(9): 1513.

Zhu, H., Zhang, M., Cai, S., Cai, Y., Wang, P., Bao, S., Zou, M., Du, M. 2014. *In situ* growth of Rh nanoparticles with controlled sizes and dispersions on the cross-linked PVA–PEI nanofibers and their electrocatalytic properties towards H_2O_2. RSC Advances 4(2): 794-804.

Zhuang, Y., Yu, F., Chen, H., Zheng, J., Ma, J., Chen, J. 2016. Alginate/graphene double-network nanocomposite hydrogel beads with low-swelling, enhanced mechanical properties, and enhanced adsorption capacity. Journal of Materials Chemistry A 4(28): 10885-10892.